AD-A112 095 NAVAL SURFACE WEAPONS CENTER DAHLGREN VA F/6 8/10
NOTES ON ESTIMATING THE SEAMOUNT SLOPE FROM VERTICAL DEFLECTION--ETC(U)
SEP 81 W J GROEGER
UNCLASSIFIED NSWC-TR-81-202 NL

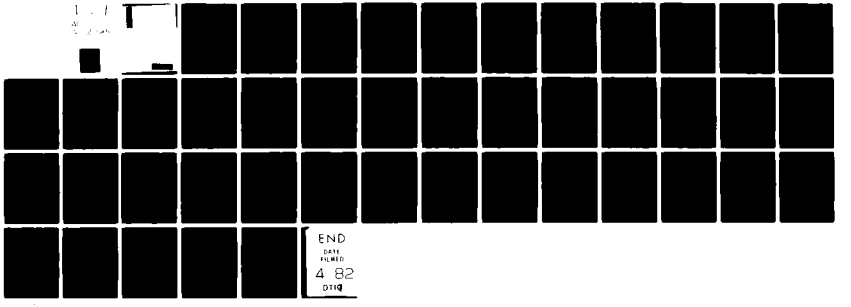

END
DATE FILMED
4 82
DTIC

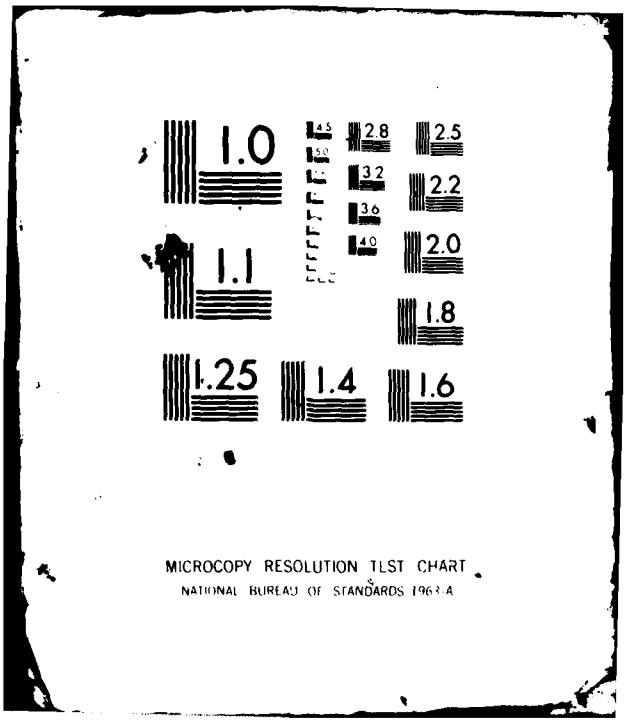
1.0
1.1
1.25
1.4
1.6
2.8
3.2
3.6
4.0
2.5
2.2
2.0
1.8
MICROCOPY RESOLUTION TEST CHART
NATIONAL BUREAU OF STANDARDS 1963-A

UNCLASSIFIED

SECURITY CLASSIFICATION OF THIS PAGE *(When Data Entered)*

REPORT DOCUMENTATION PAGE	READ INSTRUCTIONS BEFORE COMPLETING FORM
1. REPORT NUMBER: NSWC TR 81-202 — 2. GOVT ACCESSION NO.: AD-A112095	3. RECIPIENT'S CATALOG NUMBER:
4. TITLE *(and Subtitle)*: NOTES ON ESTIMATING THE SEAMOUNT SLOPE FROM VERTICAL DEFLECTION	5. TYPE OF REPORT & PERIOD COVERED: Final
	6. PERFORMING ORG. REPORT NUMBER:
7. AUTHOR(s): Walter J. Groeger	8. CONTRACT OR GRANT NUMBER(s):
9. PERFORMING ORGANIZATION NAME AND ADDRESS: Naval Surface Weapons Center (K12), Dahlgren, Virginia 22448	10. PROGRAM ELEMENT, PROJECT, TASK AREA & WORK UNIT NUMBERS: 63701B
11. CONTROLLING OFFICE NAME AND ADDRESS: Headquarters, Defense Mapping Agency, Washington, DC 20360	12. REPORT DATE: September 1981
	13. NUMBER OF PAGES: 47
14. MONITORING AGENCY NAME & ADDRESS*(if different from Controlling Office)*:	15. SECURITY CLASS. *(of this report)*: UNCLASSIFIED
	15a. DECLASSIFICATION/DOWNGRADING SCHEDULE:

16. DISTRIBUTION STATEMENT *(of this Report)*

Approved for public release; distribution unlimited.

17. DISTRIBUTION STATEMENT *(of the abstract entered in Block 20, if different from Report)*

18. SUPPLEMENTARY NOTES

19. KEY WORDS *(Continue on reverse side if necessary and identify by block number)*

Seamount Survey
Seamount model parameter estimation
Satellite radar altimetry
Ocean geodesy

20. ABSTRACT *(Continue on reverse side if necessary and identify by block number)*

Four different values of ocean depth, five seamount peak submergence depths, and various typical seamount slope angles were assumed to study the relationship between seamount slope and maximum vertical deflection (signature slope). Also, the width of the seamount at the base was compared to the signature width. The results suggest that seamount width may be inferred from the geoid height feature associated with the seamount more accurately than seamount slope.

DD FORM 1 JAN 73 1473 EDITION OF 1 NOV 65 IS OBSOLETE
S/N 0102-LF-014-6601

UNCLASSIFIED

SECURITY CLASSIFICATION OF THIS PAGE *(When Data Entered)*

FOREWORD

This study is preliminary to the design of an operational seamount detector computer algorithm for use with full coverage SEASAT-A type satellite radar altimetry. The study investigates the initializing of the seamount model parameter estimator. Because of restricted computer access, the parameter excursion is quite limited, but the initial results clarify the subject sufficiently for the immediate purpose.

The author would like to acknowledge Dr. B. Zondek of the Space and Surface Systems Division who contributed both models for the gravitational interaction of the seamount and the seamount root with the sea surface. The first seamount model is that on which the parameter estimation in the experimental (preliminary) seamount detector is based. The second seamount model (***disk model***) with which the present study was done was made available to the author in the form of a binary computer card deck with detailed operating instructions. It had been coded by R. Gordon Barker of the Physical Sciences Software Branch.

The study was undertaken in the Space and Surface Systems Division and was funded as part of the development of computer programs connected with the evaluation of seamount survey techniques.

This report was reviewed by Ralph L. Kulp, Head, Space and Ocean Geodesy Branch.

Released by:

R. T. RYLAND, JR., Head
Strategic Systems Depart.

CONTENTS

INTRODUCTION

Seamounts produce perturbations of the mean sea level (ocean surface) that are readily detectable by satellite radar altimetry. In turn, it appears that radar altimetry makes it possible to identify, locate, and survey seamounts. In particular, if the depth of the seamount peak could be inferred from the seamount's geoid height signature, submarine navigation would become less hazardous. To actually determine the feasibility of utilizing radar altimetry for a seamount survey, an effort is being made to write a computer algorithm capable of automatically recognizing the presence of seamount related perturbations among the various features of the SEASAT-A altimetry data tracks.

A two-step approach is being taken to create this algorithm. It is expected to accumulate experience and gain a first-look capability from the comparatively simple, "preliminary," seamount detector[1] that was just completed. A number of computer runs have already accomplished detections of known seamounts as well as rejections of altimetry features not related with seamounts; others are in progress. Capitalizing on these results, a more ambitious, "operational," detector algorithm is now being designed. This will be capable of processing the existing plus any future SEASAT-A type, full coverage radar altimetry with the expectation of precision results.

Essentially, both seamount detectors feature a digital filter necessary to recognize and enhance the seamount "signatures" concealed among the radar altimetry data (geoid height and vertical deflection), a physical model[2] containing the seamount related potential theory, and a mathematical mechanism that estimates the physical seamount parameters, in particular the peak submergence depth, while adjusting the characteristic properties of the radar altimetry signature predicted from the theoretical model to those extracted from the empirical data. The two seamount detectors differ in the details of the solution for the seamount model parameters. Specifically, the preliminary version is founded on the assumption that the seamount slope is proportional to the maximal vertical deflection of the associated geoid height signature. Keeping this slope angle constant throughout the procedure and applying the just mentioned seamount model,[2] the algorithm then iteratively varies the remaining seamount dimensions (width at the base, peak submergence depth) until the computed maximal geoid deviation above the seamount peak matches the altimetry signature height within a specified margin, attributing the resulting peak depth and base width to the actual seamount. Because of our very imperfect knowledge of the conditions of the crust and upper mantle underneath seamounts (problem of seamount compension), this procedure is executed twice for each detection, separately for the cases of perfect isostasy and absence of any root. The actual depth value is assumed to be bracketed by the depth estimates resulting from the two ideal cases.

The weak point of the preliminary seamount detector is not so much the simplicity of its seamount model (this being capable of calculating the geoid deflection resulting from the presence of the seamount on the seamount's symmetry axis only) but rather the empirical formula inferring the slope of the seamount from that of the sea surface above. This formula had been

devised by scrutinizing several GEOS-3 radar altimetry data tracks crossing seamounts in the New England seamount province. The study was confined to that part of the world because a dense net of altimetry tracks and reliable bathymetry were both available there. As part of the work preparatory to the design of the operational detector algorithm, the validity of this formula was re-investigated under more general conditions than those prevailing in the Western North Atlantic. Although it was still impossible to find an equally useful combination of reliable bathymetry and sufficiently dense satellite tracks (especially for SEASAT-A) elsewhere in the oceans, a new slope angle study became possible because a new seamount model had in the meantime become available.[3] This permits simulation of the geoid shape above seamount and seamount root as the combined effect of a collection of gravitating disks, the center positions, dimensions, and densities of which may be individually specified. Most importantly, this new computer program can compute geoid height and vertical deflection above the seamount along specified straight surface tracks that may pass through the seamount symmetry axis or be offset from it.

To study the relationship between seamount slope and maximal vertical deflection under wider parameter excursion than previously, four drastically differing values of ocean depth, five seamount peak submergence depths, and various typical slope angles were now assumed. For each of the altogether 60 different model seamounts, each consisting of 20 disks, the maximal signature slope was calculated and compared with the assumed seamount slope angle. In addition, the assumed width of the seamount at the base was compared to the signature width. Both sets of results are expected to be reflected in the planned operational seamount detector and to substantially improve the accuracy of its peak depth estimation over that of the present preliminary detector algorithm.

CALCULATION OF THE SEAMOUNT DISK MODEL PARAMETERS

To calculate the geoid elevation and vertical deflection, caused by the gravitational action of the model seamount and its root, along a surface track, it is expedient to approximate the seamount and the associated root by a collection of gravitating disks. The physical parameters of these disks, required by the seamount disk model computer program, are the density excess, $\Delta\rho_S = \rho_S - \rho_W$, in gr/cm^3 of the seamount disk over water and the density excess, $\Delta\rho_R = \rho_R - \rho_M$, in gr/cm^3 of the seamount root disk over the upper mantle rock. Note that the first of the two quantities is positive; the second is negative. Also needed are the disk thickness ΔS or ΔR in meters (ΔS and $\Delta R \ll R_i$), the disk radius R_i in meters, the x and y coordinates, a_i and b_i, of the disk center in meters, and, finally, the depth d_i, in meters, of the center plane of the individual disk (plane through the disk center of gravity) below the surface.

Up to 50 disks are permitted. For the purpose of this study, the seamount and the seamount root were approximated by 10 disks each. Seamounts as well as roots were assumed to be conical and mutually coaxial ($a_i = b_i = 0$). That permitted the overall properties of the seamounts and roots to conform with the geometry of the first Zondek seamount model[2] and to be mathematically manipulated by the convenient geometrical relationships of that latter model. Accordingly, the relationships among seamount width at the base, $W_S = 2\,B_S$; seamount slope angle, φ_S; seamount height, H_S; seamount peak submergence depth, d_S; and ocean depth, D, as well as seamount root width $2\,B_R$, root height H_R and crustal thickness T conform to the geometry expressed in Figure 1 (see also Reference 2). Note that for cases with isostatic compensation H_R is determined by H_S as specified in Reference 2, while for general compensation H_R may be chosen arbitrarily. The uncompensated case (absence of root) is of course characterized by $H_R = 0$ (no root disks).

For use with the present study, each of the 60 model seamounts was specified by a set of values for H_R, d_S and φ_S. From these, the remaining overall dimensions of each seamount and root were calculated according to the geometry of Figure 1. For the isostatic cases, only d_S and φ_S needed to be preselected. H_R automatically resulted from d_S and φ_S via H_S. While the ocean depth was varied over four typical values, seamount depth over five and slope angle over four, only one nominal crustal thickness was considered because of the paucity of detailed data on seamount compensation. For similar reasons, all four density figures are nominal. In accordance with Reference 2, seamount base width and width of root were considered equal ($B_S = B_R$) for the isostatic cases. For the generally compensated cases, the root width was assumed to be twice the seamount width ($B_R = sk\,B_S$; $sk = 2$) to allow for possible root genesis by plate bending.

The seamount disk parameters were then calculated according to the geometry of Figure 2.

$$d_i = D - (i - 1)\,\frac{H_S}{NS} \tag{201}$$

$$a_i = b_i = 0 \tag{202}$$

$$R_i = B_S - (i - 1)\,\frac{H_S}{NS \tan \varphi_S} = \left(1 - \frac{i - 1}{NS}\right)\frac{H_S}{\tan \varphi_S} \tag{203}$$

$$\Delta_i = \Delta_S = \frac{H_S}{NS} \tag{204}$$

$$\Delta\rho_i = \Delta\rho_S = \rho_S - \rho_W \tag{205}$$

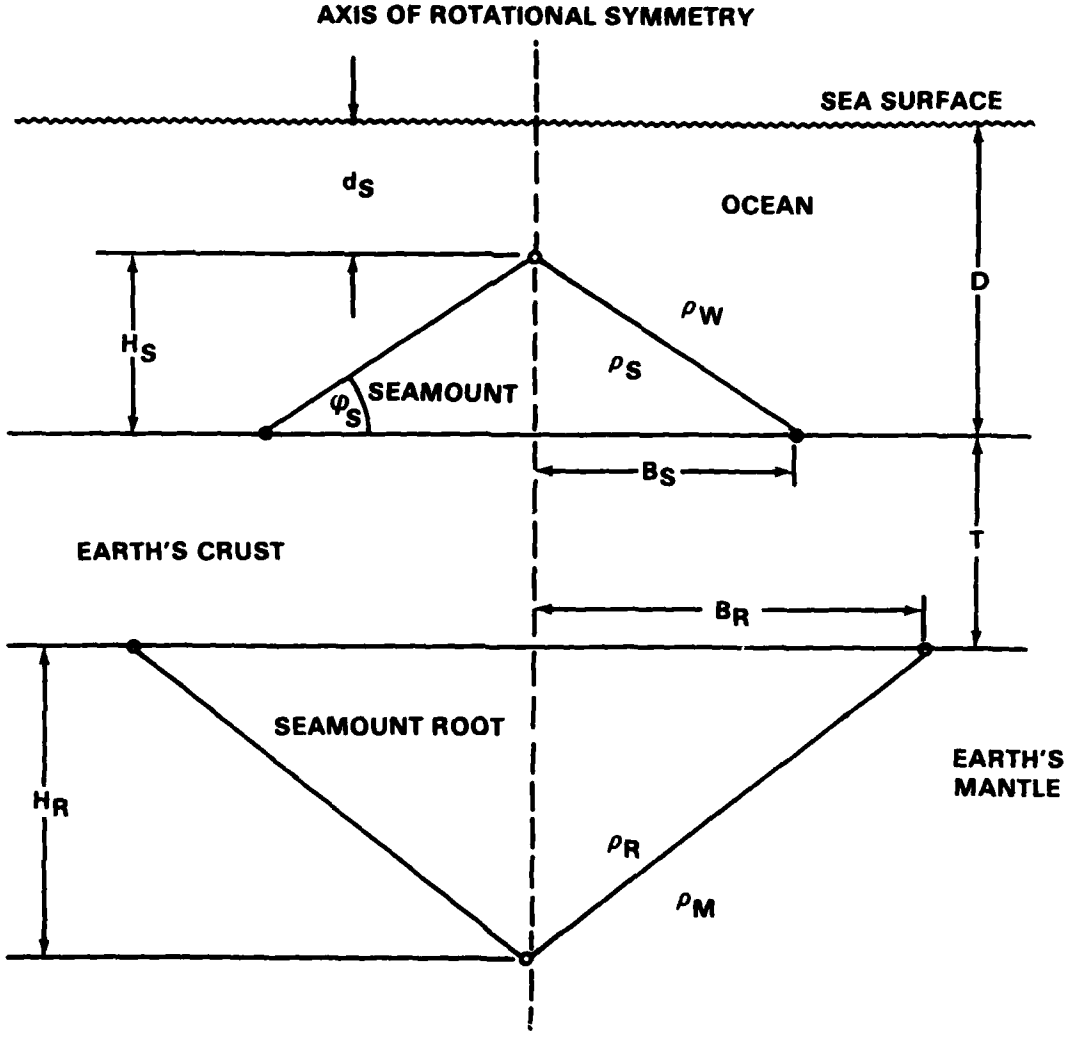

Figure 1. Geometry of the First Zondek Seamount Model

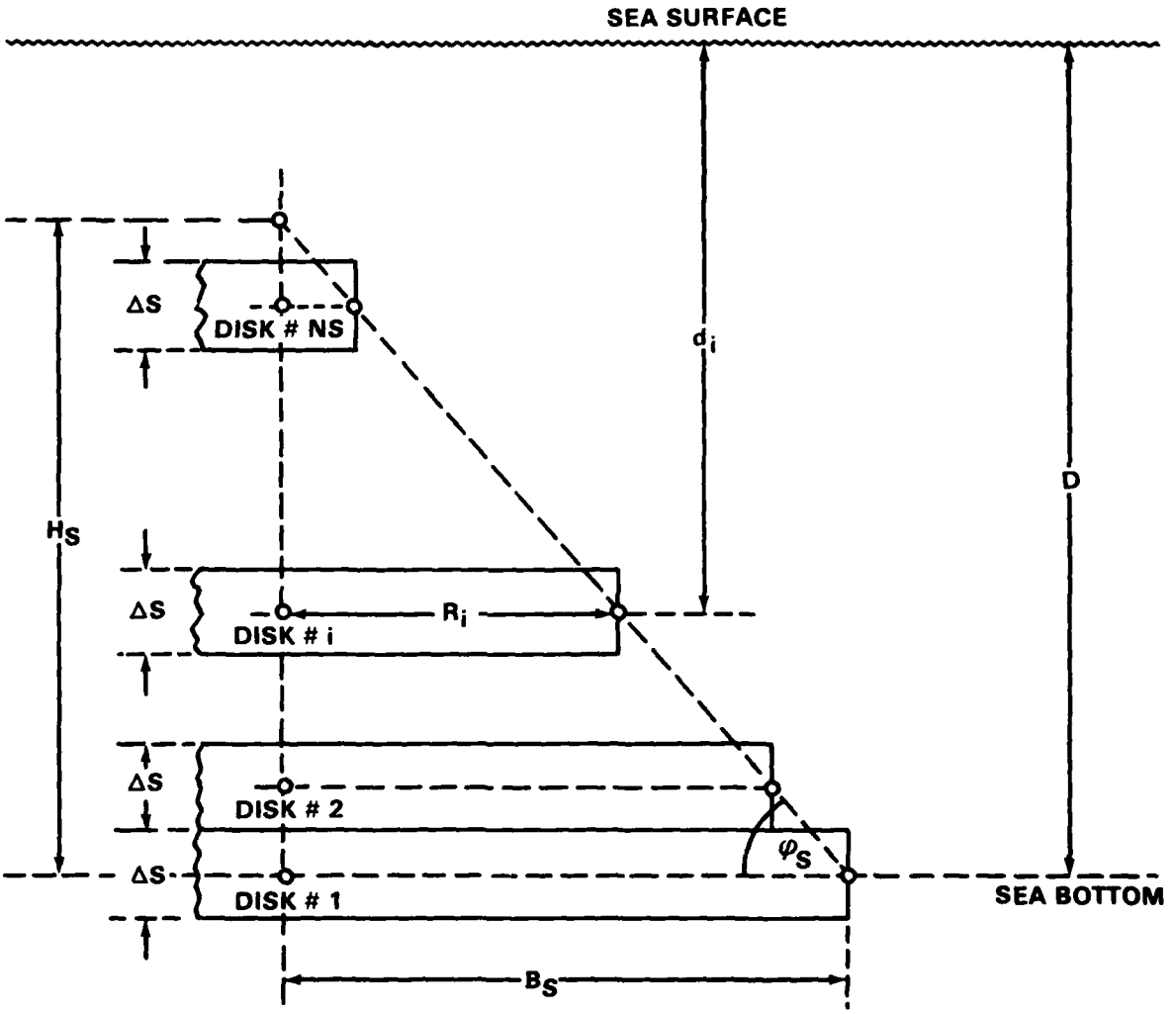

Figure 2. Geometry of the Seamount in the Seamount Disk Model

The root disk dimensions, where needed, were obtained from Figure 3.

$$d_i = D + T + (i-1)\,\Delta_R$$

$$= D + T + (i-1)\,\frac{H_R}{NR} \tag{206}$$

$$a_i = b_i = 0 \tag{207}$$

$$R_i = B_R - (i-1)\,\frac{H_R}{NR \tan \varphi_R}$$

$$= \left(1 - \frac{i-1}{NR}\right)\frac{H_R}{\tan \varphi_R} \tag{208}$$

$$\Delta_i = \Delta R = \frac{H_R}{NR} \tag{209}$$

$$\Delta\rho_i = \Delta\rho_R = \rho_R - \rho_M \tag{210}$$

For isostasy,

$$sk = 1 \rightarrow B_R = B_S \tag{211}$$

$$H_R = \left|\frac{\Delta\rho_S}{\Delta\rho_R}\right| H_S \tag{212}$$

$$\tan \varphi_R = \frac{H_R}{B_R} \tag{213}$$

For general compensation,

$$sk \geq 1 \tag{214}$$

in particular, for the present cases, sk = 2 as mentioned above. Also, H_R will be specified.

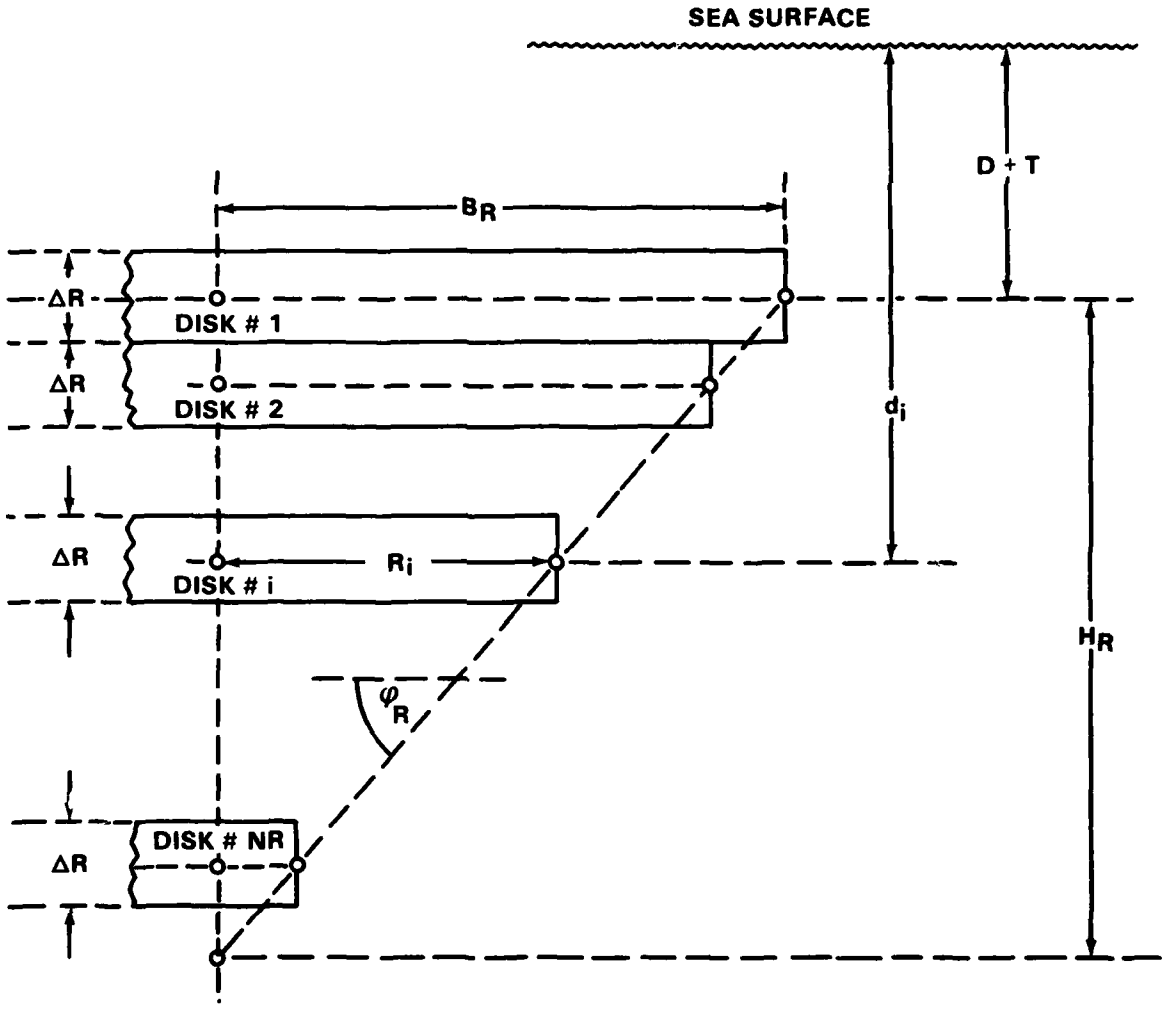

Figure 3. Geometry of the Seamount Root in the Seamount Disk Model

COMPARISON OF THE PROPERTIES OF SIMULATED SEAMOUNT SIGNATURES WITH SEAMOUNT MODEL PARAMETERS

Seamount signatures are elevations of the sea surface caused by the fact that the latter is (except for certain local or minor perturbations) an equipotential surface in the earth's gravity field. As such, its normal has the direction of the gravity vector that in the proximity of a seamount is tilted toward the seamount center of gravity.

Being artifacts of seamount gravitation, surface elevations of this type must reflect the seamount properties. Scrutiny of known seamount bathymetry and actual satellite altimetry suggests that signature width, height, and maximal value of vertical deflection are particularly useful parameters. Figure 4 represents a typical seamount signature. Note that "signature" means the twin data track consisting of the geoid height N(x) and the vertical deflection $\delta(x)$, x being the coordinate indicating the position of the satellite "footprint" on the suborbital satellite track. Let the points A and B indicate zero curvature (maximal slope) or N(x) and let P be the signature peak. Naturally, $N(x_p) = N_P = N_{SM}$ will then be the signature "height." As a measure of signature "width," the distance between A and B, $[x_B - x_A] = [x(\delta_B) - x(\delta_A)]$, will serve as well as any other meaningful convention.

According to the stated purpose of this study, a collection of about 60 model seamounts was assembled so that the individual specimen would be typical of seamounts encountered during a seamount survey using actual, SEASAT-A type, satellite altimetry. Specifically, the seamount models selected were classified and specified in terms of type and degree of compensation, peak depth d_S, and slope angle φ_S. For each specimen thus characterized, the half width B_S at the base and the maximal geoid height deflection DN_S, caused by the seamount, as well as DN_R, produced by the root, and $DN = DN_S + DN_R$ were calculated from the first Zondek seamount model according to Reference 2. Also calculated were the 20 seamount and root disks. Subsequently, for each specimen model seamount, the seamount disk model computer program was exercised with zero satellite track offset from the seamount center, resulting in values for signature half width, $(x_B - x_{SM}) = (x_{SM} - x_A)$,* geoid elevation above seamount peak, N_{SM}, and maximal vertical deflection δ_B ($/\delta_B/ = /\delta_A/$ because of model symmetry). Calculated from the latter was then the seamount slope angle, φ_{ESTIM}, using the estimator formula** from Reference 1. And finally were obtained the relative change in the signature heights resulting from the two seamount models (as a check on the mutual compatibility of the models), the ratio of signature half width to seamount half width at the base and the relative error in seamount slope angle estimation. All these are documented in Tables 1a through 4c. Note that for all tables the crustal thickness, T, is 5000 m. $\Delta\rho_S = 1.57$ gr/m^3 and $\Delta\rho_R = -0.45$ gr/cm^3.

---

*Note that both seamount models are symmetric in x with respect to the seamount center (peak).

**$(\varphi_{ESTIM})_{A,B} = \dfrac{\pi(1.5E+05)}{180 \times 3600}\,\delta_{A,B}$

Input $\delta_{A,B}$ in arc sec to obtain φ_{ESTIM} in decimal degrees.

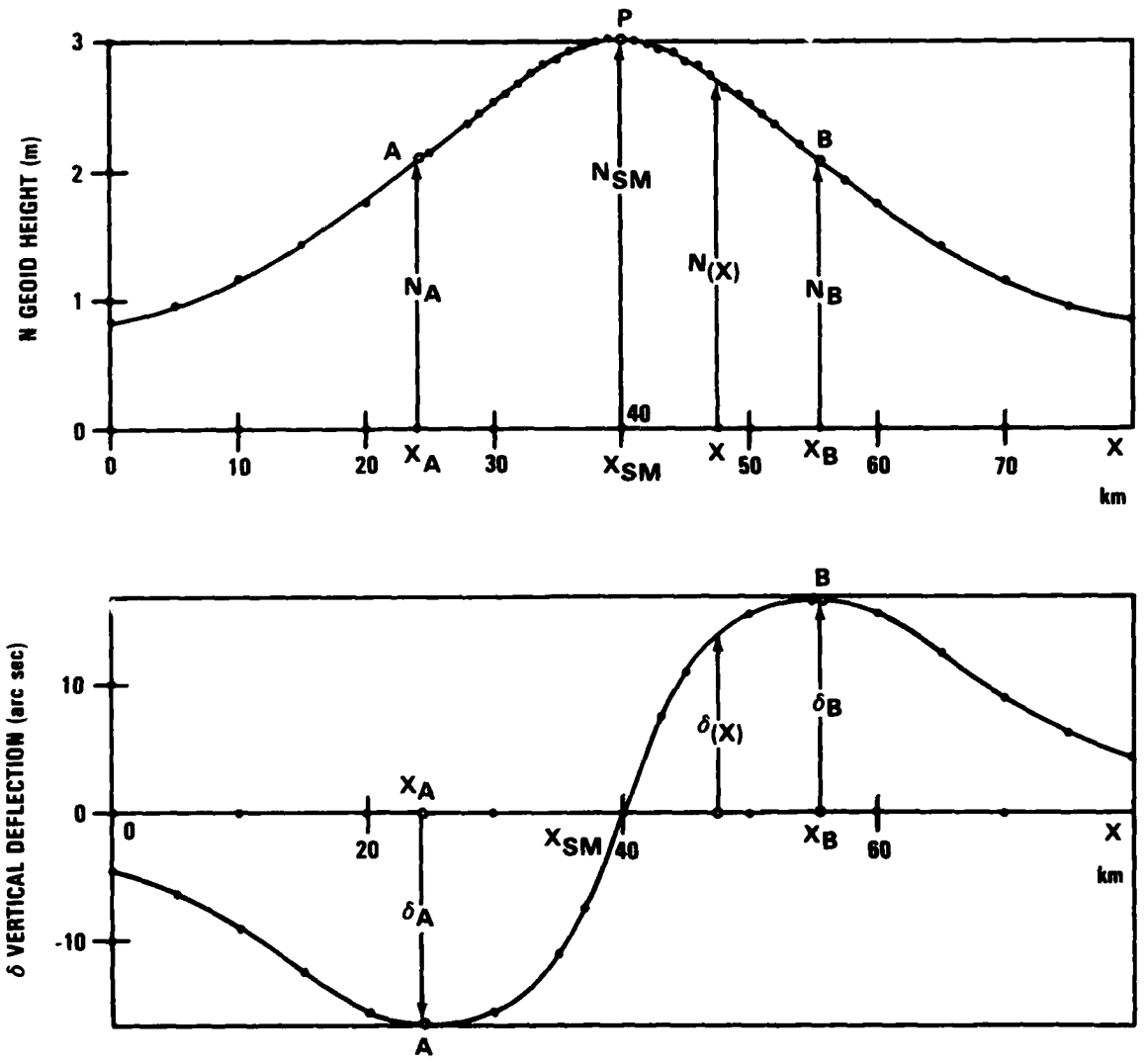

Figure 4. Typical Geoid Height Pattern and Vertical Deflection Above a Seamount

Table 1a. Parameters of Model Seamounts and Related Maximal Geoid Deflections for Ocean Depth D = 5000 m

Identification	Compensation	d_S (m)	φ_S (deg)	B_S (km)	DN_S (m)	DN_R (m)	DN (m)
5 U 01	UNCOMP	700	9	27.1491	3.19	0	3.19
5 U 02	UNCOMP	1000	9	25.2550	2.69	0	2.69
5 U 03	UNCOMP	1300	9	23.3609	2.24	0	2.24
5 U 04	UNCOMP	1600	9	21.4668	1.83	0	1.83
5 U 05	UNCOMP	1900	9	19.5726	1.47	0	1.47
5 I 01	ISOSTAT	700	9	27.1491	3.19	−1.83	1.36
5 I 02	ISOSTAT	1000	9	25.2550	2.69	−1.53	1.16
5 I 03	ISOSTAT	1300	9	23.3609	2.24	−1.27	0.97
5 I 04	ISOSTAT	1600	9	21.4668	1.83	−1.03	0.80
5 I 05	ISOSTAT	1900	9	19.5726	1.47	−0.82	0.65
5 I 06	ISOSTAT	1300	6	35.2032	3.67	−2.37	1.30
5 I 07	ISOSTAT	1300	9	23.3609	2.24	−1.27	0.97
5 I 08	ISOSTAT	1300	12	17.4071	1.53	−0.78	0.75
5 I 09	ISOSTAT	1300	15	13.8086	1.12	−0.52	0.60

Table 1b. Parameters of Model Seamounts and Related Signature Properties for Ocean Depth D = 5000 m

Identification	$(x_B - x_{SM})$ (km)	N_{SM} (m)	δ_B (arc sec)	φ_{ESTIM} (deg)	$\frac{N_{SM} - DN}{DN}$ (%)	$\frac{x_B - x_{SM}}{B_S} = \eta$	
5 U 01	16.5337	3.51	18.080	13.15	10	0.609	AVG = 0.620
5 U 02	15.3750	3.02	16.287	11.84	12	0.609	
5 U 03	14.4600	2.48	14.453	10.51	11	0.619	SDEV = 0.012
5 U 04	13.4238	2.03	12.680	9.22	11	0.625	$\frac{SDEV}{AVG} = 2\%$
5 U 05	12.4643	1.61	10.893	7.92	10	0.637	
5 I 01	12.6125	1.41	11.446	8.32	4	0.465	AVG = 0.495
5 I 02	12.1104	1.20	10.353	7.53	3	0.480	
5 I 03	11.5357	1.01	9.278	6.75	4	0.494	SDEV = 0.024
5 I 04	10.9353	0.84	8.218	5.98	5	0.509	$\frac{SDEV}{AVG} = 5\%$
5 I 05	10.2957	0.68	7.176	5.22	5	0.526	
5 I 06	15.8478	1.34	8.757	6.37	3	0.450	AVG = 0.500
5 I 07	11.5357	1.01	9.278	6.75	4	0.494	
5 I 08	9.0282	0.79	9.054	6.58	5	0.519	SDEV = 0.038
5 I 09	7.4167	0.63	8.479	6.17	5	0.537	$\frac{SDEV}{AVG} = 8\%$

Table 1c. Parameters of Model Seamounts and Related Signature Properties for Ocean Depth D = 5000 m (Continued)

Identification	$\frac{\varphi_{ESTIM} - \varphi_S}{\varphi_S}$ (%)
5 U 01	46
5 U 02	32
5 U 03	17
5 U 04	2
5 U 05	−12
5 I 01	−8
5 I 02	−16
5 I 03	−25
5 I 04	−34
5 I 05	−35
5 I 06	6
5 I 07	−25
5 I 08	−45
5 I 09	−59

Table 2a. Parameters of Model Seamounts and Related Maximal Geoid Deflections for Ocean Depth D = 4000 m

Identification	Compensation	d_S (m)	φ_S (deg)	B_S (km)	DN_S (m)	DN_R (m)	DN (m)
4 U 01	UNCOMP	700	9	20.8354	1.850	0	1.850
4 U 02	UNCOMP	1000	9	18.9413	1.478	0	1.478
4 U 03	UNCOMP	1300	9	17.0471	1.515	0	1.515
4 U 04	UNCOMP	1600	9	15.1530	0.867	0	0.867
4 U 05	UNCOMP	1900	9	13.2589	0.625	0	0.625
4 I 01	ISOSTAT	700	9	20.8354	1.850	−1.003	0.848
4 I 02	ISOSTAT	1000	9	18.9413	1.478	−0.793	0.686
4 I 03	ISOSTAT	1300	9	17.0471	1.151	−0.609	0.541
4 I 04	ISOSTAT	1600	9	15.1530	0.867	−0.452	0.415
4 I 05	ISOSTAT	1900	9	13.2589	0.625	−0.320	0.305
4 I 06	ISOSTAT	1300	6	25.6888	1.908	−1.168	0.740
4 I 07	ISOSTAT	1300	9	17.0471	1.151	−0.609	0.541
4 I 08	ISOSTAT	1300	12	12.7025	0.781	−0.370	0.411
4 I 09	ISOSTAT	1300	15	10.0765	0.565	−0.245	0.320
4 G 01	GENERAL *	700	9	20.8354	1.850	−0.437	1.414
4 G 02	GENERAL *	1000	9	18.9413	1.478	−0.384	1.094
4 G 03	GENERAL *	1300	9	17.0471	1.151	−0.332	0.818
4 G 04	GENERAL *	1600	9	15.1530	0.867	−0.282	0.585
4 G 05	GENERAL *	1900	9	13.2589	0.625	−0.232	0.393

* sk = 2; H_R = 1600 m

Table 2b. Parameters of Model Seamounts and Related Signature Properties for Ocean Depth D = 4000 m

Identification	$(x_B - x_{SM})$ (km)	N_{SM} (m)	δ_B (arc sec)	φ_{ESTIM} (deg)	$\frac{N_{SM} - DN}{DN}$ (%)	$\frac{x_B - x_{SM}}{B_S} = \eta$	
4 U 01	12.7456	2.043	13.603	9.89	10	0.612	AVG = 0.628
4 U 02	11.7083	1.635	11.793	8.58	11	0.618	
4 U 03	10.6783	1.275	10.020	7.29	11	0.626	SDEV = 0.015
4 U 04	9.6407	0.962	8.292	6.03	11	0.636	$\frac{SDEV}{AVG}$ = 2%
4 U 05	8.6079	0.696	6.625	4.82	11	0.649	
4 I 01	10.2217	0.884	9.055	6.59	4	0.491	AVG = 0.529
4 I 02	9.6134	0.718	7.949	5.78	5	0.508	
4 I 03	8.9907	0.570	6.858	4.99	5	0.527	SDEV = 0.031
4 I 04	8.3000	0.438	5.782	4.21	6	0.548	$\frac{SDEV}{AVG}$ = 6%
4 I 05	7.5593	0.325	4.722	3.43	7	0.570	
4 I 06	12.5652	0.772	6.646	4.83	4	0.489	AVG = 0.535
4 I 07	8.9907	0.570	6.858	4.99	5	0.527	
4 I 08	7.0027	0.433	6.520	4.74	5	0.551	SDEV = 0.036
4 I 09	5.7653	0.341	5.954	4.33	7	0.572	$\frac{SDEV}{AVG}$ = 7%
4 G 01	12.1991	1.553	12.600	9.16	10	0.586	AVG = 0.598
4 G 02	11.1777	1.204	10.845	7.89	10	0.590	
4 G 03	10.1589	0.901	9.133	6.64	10	0.596	SDEV = 0.011
4 G 04	9.1795	0.645	7.477	5.44	10	0.606	$\frac{SDEV}{AVG}$ = 2%
4 G 05	8.1164	0.434	5.888	4.28	10	0.612	

Table 2c. Parameters of Model Seamounts and Related Signature Properties for Ocean Depth D = 4000 m (Continued)

Identification	$\frac{\varphi_{ESTIM}-\varphi_S}{\varphi_S}$ (%)
4 U 01	10
4 U 02	− 5
4 U 03	−19
4 U 04	−33
4 U 05	−46
4 I 01	−27
4 I 02	−36
4 I 03	−45
4 I 04	−53
4 I 05	−62
4I 06	−20
4 I 07	−45
4 I 08	−61
4 I 09	−71
4 G 01	2
4 G 02	−12
4 G 03	−26
4 G 04	−40
4 G 05	−52

Table 3a. Parameters of Model Seamounts and Related Maximal Geoid Deflections for Ocean Depth D = 3000 m

Identification	Compensation	d_S (m)	φ_S (deg)	B_S (km)	DN_S (m)	DN_R (m)	DN (m)
3 U 01	UNCOMP	700	9	14.5216	0.88	0	0.88
3 U 02	UNCOMP	1000	9	12.6275	0.63	0	0.63
3 U 03	UNCOMP	1300	9	10.7334	0.42	0	0.42
3 U 04	UNCOMP	1600	9	8.8393	0.26	0	0.26
3 U 05	UNCOMP	1900	9	6.9451	0.14	0	0.14
3 I 01	ISOSTAT	700	9	14.5216	0.88	−0.43	0.44
3 I 02	ISOSTAT	1000	9	12.6275	0.63	−0.30	0.33
3 I 03	ISOSTAT	1300	9	10.7334	0.42	−0.20	0.23
3 I 04	ISOSTAT	1600	9	8.8393	0.26	−0.12	0.14
3 I 05	ISOSTAT	1900	9	6.9451	0.14	−0.06	0.08
3 I 06	ISOSTAT	1300	6	16.1744	0.72	−0.40	0.32
3 I 07	ISOSTAT	1300	9	10.7334	0.42	−0.20	0.23
3 I 08	ISOSTAT	1300	12	7.9979	0.28	−0.12	0.17
3 I 09	ISOSTAT	1300	15	6.3445	0.20	−0.08	0.12

Table 3b. Parameters of Model Seamounts and Related Signature Properties for Ocean Depth D = 3000 m

Identification	$(x_B - x_{SM})$ (km)	N_{SM} (m)	δ_B (arc sec)	φ_{ESTIM} (deg)	$\frac{N_{SM} - DN}{DN}$ (%)	$\frac{x_B - x_{SM}}{B_S} = \eta$	
3 U 01	8.9625	0.97	9.133	6.64	10	0.617	AVG = 0.650
3 U 02	7.9310	0.70	7.356	5.35	11	0.628	
3 U 03	6.9000	0.47	5.643	4.10	12	0.643	SDEV = 0.032
3 U 04	5.8822	0.29	4.024	2.93	12	0.665	$\frac{SDEV}{AVG}$ = 5%
3 U 05	4.8432	0.16	2.550	1.85	14	0.697	
3 I 01	7.6374	0.47	6.575	4.78	7	0.526	AVG = 0.582
3 I 02	6.9497	0.35	5.425	3.95	6	0.550	
3 I 03	6.1882	0.24	4.285	3.12	4	0.577	SDEV = 0.048
3 I 04	5.3447	0.16	3.159	2.30	14	0.605	$\frac{SDEV}{AVG}$ = 8%
3 I 05	4.5126	0.09	2.078	1.51	13	0.650	
3 I 06	8.8056	0.34	4.419	3.21	6	0.544	AVG = 0.590
3 I 07	6.1882	0.24	4.285	3.12	4	0.577	
3 I 08	4.8266	0.18	3.845	2.80	6	0.604	SDEV = 0.039
3 I 09	4.0287	0.14	3.339	2.43	17	0.635	$\frac{SDEV}{AVG}$ = 7%

Table 3c. Parameters of Model Seamounts and Related Signature Properties for Ocean Depth D = 3000 m (Continued)

Identification	$\frac{\varphi_{ESTIM}-\varphi_S}{\varphi_S}$ (%)
3 U 01	−26
3 U 02	−41
3 U 03	−54
3 U 04	−67
3 U 05	−79
3 I 01	−47
3 I 02	−56
3 I 03	−65
3 I 04	−74
3 I 05	−83
3 I 06	−47
3 I 07	−65
3 I 08	−77
3 I 09	−84

Table 4a. Parameters of Model Seamounts and Related Maximal Geoid Deflections for Ocean Depth D = 2000 m

Identification	Compensation	d_S (m)	φ_S (deg)	B_S (km)	DN_S (m)	DN_R (m)	DN (m)
2 U 01	UNCOMP	700	9	8.2079	0.263	0	0.263
2 U 02	UNCOMP	1000	9	6.3138	0.139	0	0.139
2 U 03	UNCOMP	1300	9	4.4196	0.056	0	0.056
2 U 04	UNCOMP	1600	9	2.5255	0.013	0	0.013
2 U 05	UNCOMP	1900	9	–	–	–	–
2 I 01	ISOST	700	9	8.2079	0.263	−0.106	0.157
2 I 02	ISOST	1000	9	6.3138	0.139	−0.052	0.087
2 I 03	ISOST	1300	9	4.4196	0.056	−0.019	0.037
2 I 04	ISOST	1600	9	2.5255	0.013	−0.004	0.009
2 I 05	ISOST	1900	9	–	–	–	–
2 I 06	ISOST	1300	9	6.6601	0.012	−0.041	0.060
2 I 07	ISOST	1300	9	4.4196	0.056	−0.019	0.037
2 I 08	ISOST	1300	12	3.2932	0.035	−0.011	0.025
2 I 09	ISOST	1300	15	2.6124	0.024	−0.007	0.017

Table 4b. Parameters of Model Seamounts and Related Signature Properties for Ocean Depth D = 2000 m

Identification	$(x_B - x_{SM})$ (km)	N_{SM} (m)	δ_B (arc sec)	φ_{ESTIM} (deg)	$\frac{N_{SM} - DN}{DN}$ (%)	$\frac{x_B - x_{SM}}{B_S} = \eta$	
2 U 01	5.2264	0.291	4.690	3.41	11	0.637	AVG = 0.713
2 U 02	4.1780	0.154	3.009	2.19	11	0.662	
2 U 03	3.2086	0.063	1.527	1.11	13	0.726	SDEV = 0.084
2 U 04	2.0873	0.014	0.426	0.31	8	0.826	$\frac{SDEV}{AVG} = 12\%$
2 U 05	–	–	–	–	–	–	
2 I 01	4.7700	0.170	3.842	2.79	8	0.581	AVG = 0.700
2 I 02	3.9296	0.094	2.566	1.87	8	0.622	
2 I 03	3.0758	0.041	1.361	0.99	11	0.696	SDEV = 0.142
2 I 04	2.2756	0.010	0.404	0.29	11	0.901	$\frac{SDEV}{AVG} = 20\%$
2 I 05	–	–	–	–	–	–	
2 I 06	4.2345	0.066	1.739	1.26	10	0.636	AVG = 0.738
2 I 07	3.0758	0.041	1.361	0.99	11	0.696	
2 I 08	2.4857	0.027	1.039	0.76	13	0.755	SDEV = 0.097
2 I 09	2.2541	0.019	0.790	0.57	12	0.863	$\frac{SDEV}{AVG} = 13\%$

Table 4c. Parameters of Model Seamounts and Related Signature Properties for Ocean Depth D = 2000 m (Continued)

Identification	$\frac{\varphi_{ESTIM}-\varphi_S}{\varphi_S}$ (%)
2 U 01	−62
2 U 02	−76
2 U 03	−88
2 U 04	−97
2 U 05	–
2 I 01	−69
2 I 02	−79
2 I 03	−89
2 I 04	−97
2 I 05	–
2 I 06	−79
2 I 07	−89
2 I 08	−94
2 I 09	−96

All simulated seamount crossings discussed thus far have in common zero track offset (from the seamount symmetry axis). In operational seamount surveys, this will be an unlikely situation indeed. Apart from the fact that seamounts in the real world are rarely ever conical, even if they were, it is obvious that one will always be uncertain as to the distance by which the suborbital track misses the seamount peak when handling operational data. Although a more thorough scrutiny of the subject matter would have been desirable but was not possible because of the restrictions on access to the computer already mentioned, a quick look was taken at data that indicate the effect of miss distance on our method of seamount parameter estimation. To be precise, the disk model was exercised to produce a number of simulated geoid height and vertical deflection signatures for various track offsets, y, all for the 5000-m ocean depth that is typical for many of the world's seamounts. The results are compiled in Tables 5a through 9b.

Table 5a. Parameters of Simulated Seamount Signatures for Variable Track Offset from Seamount Peak

Identification	Compensation	d_S (m)	φ_S (deg)	y (km)	N_{SM} (m)	
5 U 01	UNCOMP	700	9	0	3.52	AVG = 2.557
				5	3.36	
				10	3.02	SDEV = 0.794
				15	2.61	
				20	2.17	$\frac{SDEV}{AVG}$ = 31%
				25	1.77	
				30	1.45	
5 U 02	UNCOMP	1000	9	0	3.02	AVG = 2.124
				5	2.87	
				10	2.52	SDEV = 0.718
				15	2.14	
				20	1.75	$\frac{SDEV}{AVG}$ = 34%
				25	1.41	
				30	1.16	
5 U 03	UNCOMP	1300	9	0	2.48	AVG = 1.714
				5	2.35	
				10	2.06	SDEV = 0.612
				15	1.72	
				20	1.38	$\frac{SDEV}{AVG}$ = 36%
				25	1.10	
				30	0.91	

Table 5b. Parameters of Simulated Seamount Signatures for Variable Track Offset from Seamount Peak (Continued)

Identification	$(x_B - x_{SM})$ (km)		δ_B (arc sec)	
5 U 01	16.534	AVG = 17.439	18.1	AVG = 11.771
	16.841		17.3	
	17.277	SDEV = 1.163	15.2	SDEV = 5.464
	17.298		12.3	
	16.912	$\frac{SDEV}{AVG} = 7\%$	9.2	$\frac{SDEV}{AVG} = 46\%$
	17.214		6.2	
	20.000		4.1	
5 U 02	15.375	AVG = 16.615	16.3	AVG = 10.157
	15.717		15.5	
	16.149	SDEV = 1.642	13.4	SDEV = 5.190
	16.116		10.5	
	15.822	$\frac{SDEV}{AVG} = 10\%$	7.4	$\frac{SDEV}{AVG} = 51\%$
	16.962		4.8	
	20.167		3.2	
5 U 03	14.460	AVG = 15.947	14.5	AVG = 8.629
	14.742		13.6	
	15.061	SDEV = 2.170	11.5	SDEV = 4.774
	14.951		8.7	
	14.938	$\frac{SDEV}{AVG} = 14\%$	5.9	$\frac{SDEV}{AVG} = 55\%$
	16.974		3.7	
	20.500		2.5	

Table 6a. Parameters of Simulated Seamount Signatures for Variable Track Offset from Seamount Peak

Identification	Compensation	d_S (m)	φ_S (deg)	y (km)	N_{SM} (m)	
5 U 04	UNCOMP	1600	9	0	2.03	AVG = 1.367
				5	1.91	
				10	1.66	SDEV = 0.520
				15	1.35	
				20	1.07	$\frac{SDEV}{AVG} = 38\%$
				25	0.85	
				30	0.70	
5 U 05	UNCOMP	1900	9	0	1.61	AVG = 1.057
				5	1.52	
				10	1.29	SDEV = 0.430
				15	1.03	
				20	0.80	$\frac{SDEV}{AVG} = 41\%$
				25	0.63	
				30	0.52	
5 I 01	ISOSTAT	700	9	0	1.41	AVG = 0.787
				5	1.29	
				10	1.05	SDEV = 0.482
				15	0.77	
				20	0.51	$\frac{SDEV}{AVG} = 61\%$
				25	0.31	
				30	0.17	

Table 6b. Parameters of Simulated Seamount Signatures for Variable Track Offset from Seamount Peak (Continued)

Identification	$(x_B - x_{SM})$ (km)		δ_B (arc sec)	
5 U 04	13.424	AVG = 15.256	12.7	AVG = 7.200
	13.684		11.8	
	13.939	SDEV = 2.621	9.7	SDEV = 4.329
	13.833		7.0	
	14.342	$\frac{SDEV}{AVG} = 17\%$	4.5	$\frac{SDEV}{AVG} = 60\%$
	17.071		2.8	
	20.500		1.9	
5 U 05	12.464	AVG = 14.693	10.9	AVG = 5.900
	12.676		10.1	
	12.844	SDEV = 3.144	8.0	SDEV = 3.844
	12.817		5.5	
	14.100	$\frac{SDEV}{AVG} = 21\%$	3.3	$\frac{SDEV}{AVG} = 65\%$
	17.200		2.1	
	20.750		1.4	
5 I 01	12.613	AVG = 13.790	11.4	AVG = 6.429
	13.340		10.6	
	14.308	SDEV = 0.715	8.7	SDEV = 4.009
	14.680		6.5	
	14.229	$\frac{SDEV}{AVG} = 5\%$	4.3	$\frac{SDEV}{AVG} = 62\%$
	13.362		2.4	
	14.000		1.1	

Table 7a. Parameters of Simulated Seamount Signatures for Variable Track Offset from Seamount Peak

Identification	Compensation	d_S (m)	φ_S (deg)	y (km)	N_{SM} (m)	
5 I 02	ISOSTAT	1000	9	0	1.20	AVG = 0.644
				5	1.09	
				10	0.87	SDEV = 0.424
				15	0.62	
				20	0.39	$\frac{SDEV}{AVG} = 66\%$
				25	0.22	
				30	0.12	
5 I 03	ISOSTAT	1300	9	0	1.01	AVG = 0.523
				5	0.91	
				10	0.71	SDEV = 0.364
				15	0.49	
				20	0.29	$\frac{SDEV}{AVG} = 70\%$
				25	0.16	
				30	0.09	
5 I 04	ISOSTAT	1600	9	0	0.84	AVG = 0.416
				5	0.75	
				10	0.57	SDEV = 0.311
				15	0.37	
				20	0.21	$\frac{SDEV}{AVG} = 75\%$
				25	0.11	
				30	0.06	

Table 7b. Parameters of Simulated Seamount Signatures for Variable Track Offset from Seamount Peak (Continued)

Identification	$(x_B - x_{SM})$ (km)		δ_B (arc sec)	
5 I 02	12.110	AVG = 13.178	10.4	AVG = 5.571
	12.747		9.5	
	13.585	SDEV = 0.712	7.7	SDEV = 3.781
	13.767		5.5	
	13.167	$\frac{SDEV}{AVG} = 5\%$	3.4	$\frac{SDEV}{AVG} = 68\%$
	12.700		1.7	
	14.167		0.8	
5 I 03	11.536	AVG = 12.593	9.3	AVG = 4.771
	12.117		8.5	
	12.815	SDEV = 0.873	6.7	SDEV = 3.509
	12.805		4.6	
	12.158	$\frac{SDEV}{AVG} = 7\%$	2.6	$\frac{SDEV}{AVG} = 74\%$
	12.423		1.2	
	14.300		0.5	
5 I 04	10.935	AVG = 11.924	8.2	AVG = 4.000
	11.444		7.4	
	12.000	SDEV = 1.298	5.7	SDEV = 3.168
	11.816		3.7	
	10.474	$\frac{SDEV}{AVG} = 11\%$	1.8	$\frac{SDEV}{AVG} = 79\%$
	12.300		0.8	
	14.500		0.4	

Table 8a. Parameters of Simulated Seamount Signatures for Variable Track Offset from Seamount Peak

Identification	Compensation	d_S (m)	φ_S (deg)	y (km)	N_{SM} (m)	
5 I 05	ISOSTAT	1900	9	0	0.68	AVG = 0.323
				5	0.60	
				10	0.44	SDEV = 0.255
				15	0.27	
				20	0.15	$\frac{SDEV}{AVG} = 79\%$
				25	0.08	
				30	0.04	
5 I 06	ISOSTAT	1300	9	0	1.34	AVG = 0.869
				5	1.27	
				10	1.10	SDEV = 0.393
				15	0.89	
				20	0.68	$\frac{SDEV}{AVG} = 45\%$
				25	0.48	
				30	0.32	
5 I 07	ISOSTAT	1300	9	0	1.01	AVG = 0.523
				5	0.91	
				10	0.71	SDEV = 0.364
				15	0.49	
				20	0.29	$\frac{SDEV}{AVG} = 70\%$
				25	0.16	
				30	0.09	

Table 8b. Parameters of Simulated Seamount Signatures for Variable Track Offset from Seamount Peak (Continued)

Identification	$(x_B - x_{SM})$ (km)		δ_B (arc sec)	
5 I 05	10.296	AVG = 11.573	7.2	AVG = 3.329
	10.747		6.4	
	11.135	SDEV = 1.575	4.7	SDEV = 2.808
	10.840		2.8	
	10.800	$\frac{SDEV}{AVG} = 14\%$	1.3	$\frac{SDEV}{AVG} = 84\%$
	12.357		0.6	
	14.833		0.3	
5 I 06	15.848	AVG = 17. 559	8.8	AVG = 5.871
	16.690		8.4	
	17.814	SDEV = 1.122	7.4	SDEV = 2.520
	18.633		6.1	
	18.845	$\frac{SDEV}{AVG} = 6\%$	4.8	$\frac{SDEV}{AVG} = 43\%$
	18.250		3.4	
	16.833		2.2	
5 I 07	11.536	AVG = 12.593	9.3	AVG = 4.771
	12.117		8.5	
	12.815	SDEV = 0.873	6.7	SDEV = 3.509
	12.805		4.6	
	12.158	$\frac{SDEV}{AVG} = 7\%$	2.6	$\frac{SDEV}{AVG} = 74\%$
	12.423		1.2	
	14.300		0.5	

Table 9a. Parameters of Simulated Seamount Signatures for Variable Track Offset from Seamount Peak

Identification	Compensation	d_S (m)	φ_S (deg)	y (km)	N_{SM} (m)	
5 I 08	ISOSTAT	1300	12	0	0.79	AVG = 0.349
				5	0.68	
				10	0.46	SDEV = 0.301
				15	0.27	
				20	0.13	$\frac{SDEV}{AVG} = 86\%$
				25	0.07	
				30	0.04	
5 I 09	ISOSTAT	1300	15	0	0.63	AVG = 0.247
				5	0.51	
				10	0.31	SDEV = 0.243
				15	0.15	
				20	0.07	$\frac{SDEV}{AVG} = 98\%$
				25	0.04	
				30	0.02	

Table 9b. Parameters of Simulated Seamount Signatures for Variable Track Offset from Seamount Peak (Continued)

Identification	$(x_B - x_{SM})$ (km)		δ_B (arc sec)	
5 I 08	9.028	AVG = 10.953	9.1	AVG = 3.843
	9.554		7.8	
	9.949	SDEV = 2.141	5.3	SDEV = 3.604
	9.821		2.8	
	10.618	$\frac{SDEV}{AVG} = 20\%$	1.2	$\frac{SDEV}{AVG} = 94\%$
	12.700		0.5	
	15.000		0.2	
5 I 09	7.417	AVG = 10.233	8.5	AVG = 3.129
	7.951		6.9	
	8.265	SDEV = 3.012	3.9	SDEV = 3.405
	8.871		1.6	
	10.625	$\frac{SDEV}{AVG} = 29\%$	0.6	$\frac{SDEV}{AVG} = 109\%$
	13.000		0.3	
	15.500		0.1	

SUMMARY

As already stated, one of the purposes of the present study is the re-investigation of the simple estimator formula used in the experimental version of the seamount detector (see Reference 1 and the footnote on Page 8 of this report). While this formula was developed from GEOS-3 altimetry in the New England seamount province and was quite accurate then (which is still reflected in the 2% figure for the relative accuracy of slope angle estimation obtained for case 5 U 04 in Table 1c), it does not show very well under the greater variety of conditions considered now. On the other hand, according to the last columns in Table 1b, 2b, 3b, and 4b representing the ratio of signature half width to seamount half width at the base, this latter quantity appears to be quite insensitive to changes in the seamount parameters and ocean depth. With $(x_B - x_{SM})$, the signature half width, known from the altimetry, it is then possible to calculate B_S, the seamount half width at the base, very simply and quite accurately. This indicates that the estimation ("measuring") of the seamount parameters ought to be based on the signature width rather than on the the signature slope angle (maximal vertical deflection). The quantitative details are illustrated in Figures 5, 6, and 7 and are expected to be useful when applied to the design of the operational seamount detector.

As far as the question of the track offset from the seamount center is concerned, the data in Tables 5a through 5e indicate that missing the center by about 10 km on either side is relatively inconsequential (the author is aware of the desirability of a comparison with the data errors introduced by the imperfect approximation of nature by the two seamount models). When admitting excursions in track offset of as much as 30 km on either side of the center, the resulting uncertainty in the signature slope angle $\delta_{A,B}$, and, consequently, the error in the estimate of the seamount slope become rather severe. At the same time, the uncertainty in the signature half width $(x_B - x_{SM})$ is comparatively limited. This is again taken to indicate that the estimation of the seamount parameters ought to start (especially if a single-parameter solution is planned as the basis of the estimator algorithm) from the signature width rather than from the signature slope.

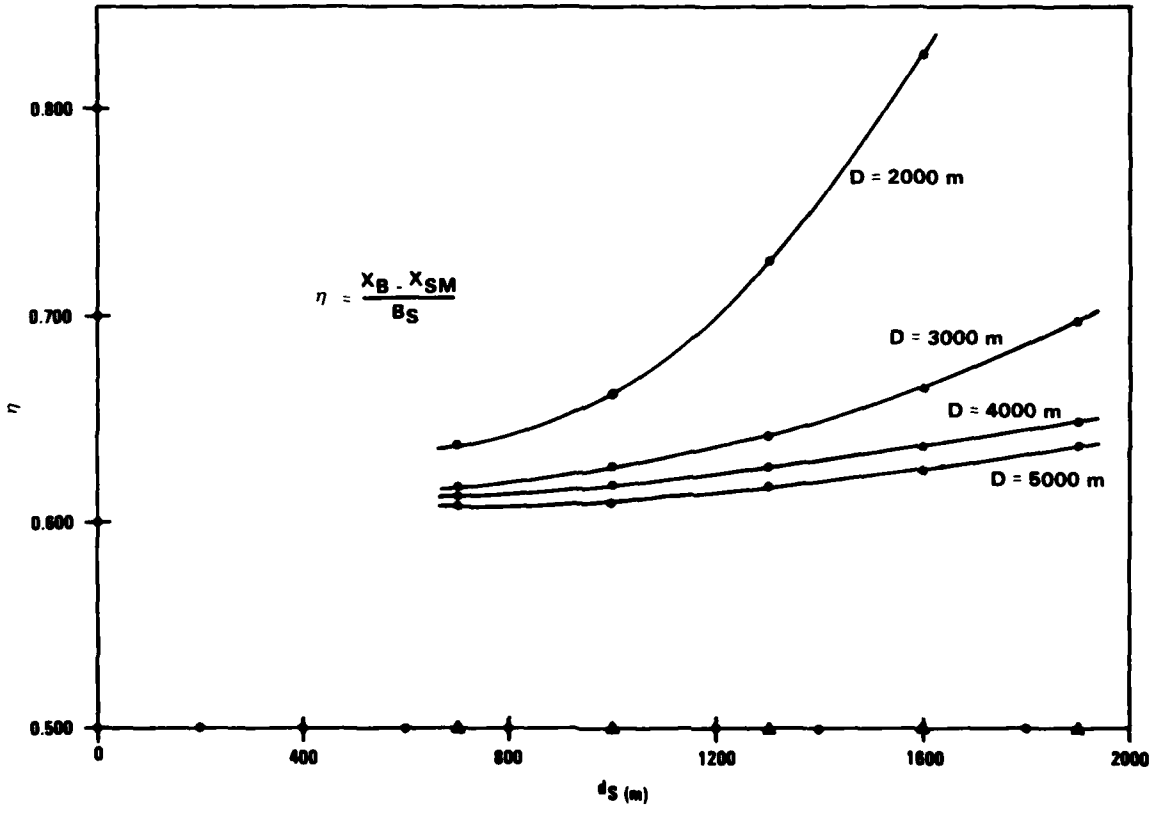

Figure 5. Ratio of Signature Width to Seamount Width at Base versus Seamount Peak Depth for Uncompensated Seamounts (Seamount Slope Angle is 9 deg)

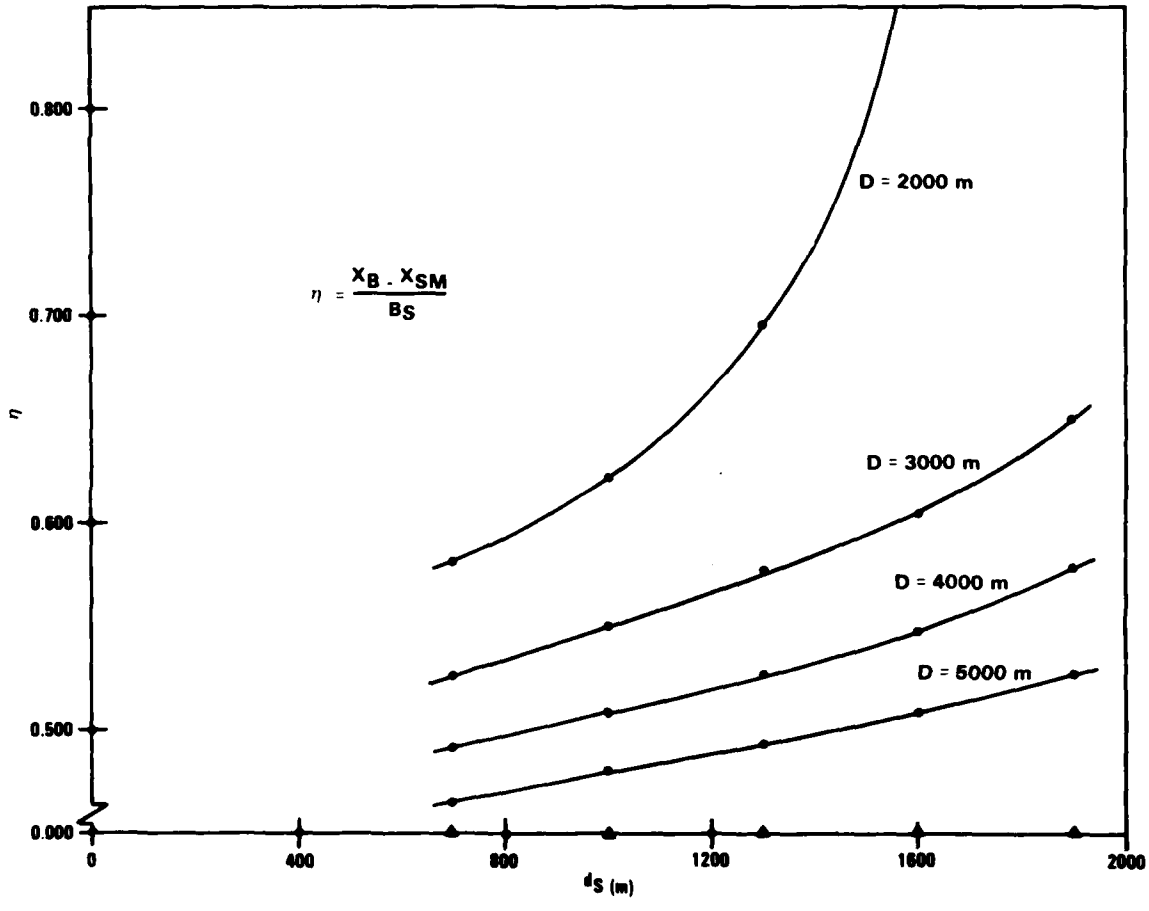

Figure 6. Ratio of Signature Width to Seamount Width at Base versus Seamount Peak Depth for Isostatically Compensated Seamounts (Seamount Slope Angle is 9 deg)

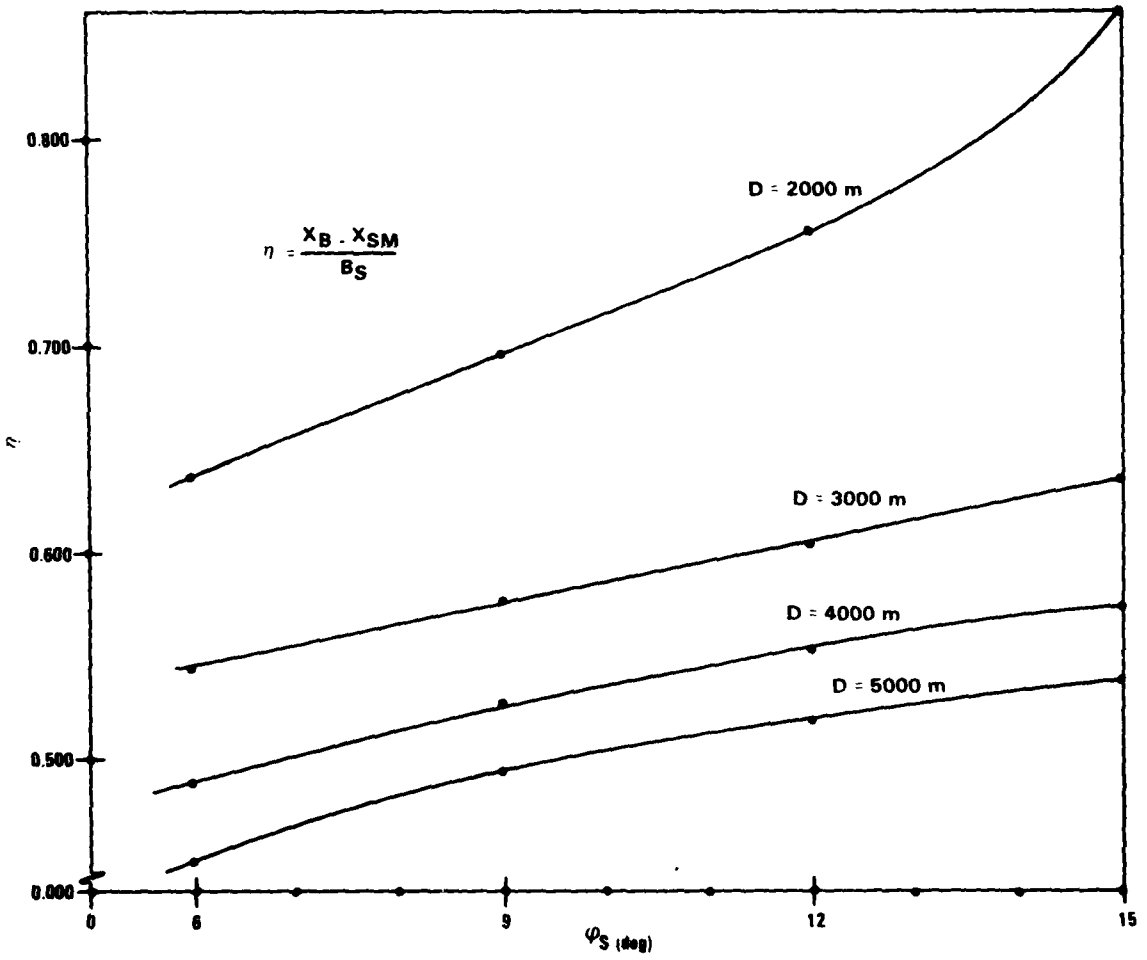

Figure 7. Ratio of Signature Width to Seamount Width at Base versus Seamount Slope Angle for Isostatically Compensated Seamounts (Depth of Seamount Peak is 1300 m)

REFERENCES

1. W. Groeger, *AN EXPERIMENTAL COMPUTER ALGORITHM FOR SEAMOUNT MODEL PARAMETER ESTIMATION BASED ON SEASAT-A SATELLITE RADAR ALTIMETRY*, NSWC TR 81-200 (Dahlgren, Virginia, September 1981).

2. B. Zondek, *MAXIMAL GEOIDAL ELEVATIONS DUE TO SIMULATED SEAMOUNTS*, NSWC/DL TR-3915 (Dahlgren, Virginia, November 1978).

3. *Seamount Disk Model*, unpublished work by Dr. B. Zonkek of the Space and Surface Systems Division.

DISTRIBUTION

Defense Mapping Agency
Naval Observatory Building 56
ATTN: O. W. Williams
C. Martin
P. M. Schwimmer
W. Senus
R. Berkowitz
Washington, DC 20360

Defense Mapping Agency
Aerospace Center
ATTN: L. B. Decker
M. Schultz
K. Nelson
St. Louis, MO 63118

Defense Mapping Agency
Hydrographic/Topographic Center
6500 Brooks Lane
ATTN: H. Heuerman
Washington, DC 20315

Defense Technical Information Center
Cameron Station
Alexandria, VA 22314 (12)

Library of Congress
ATTN: Gift and Exchange Division (4)
Washington, DC 20540

Commander
Naval Oceanographic Office
NSTL Station
ATTN: T. Davis (5)
J. Hankins
S. Odenthal
Bay St. Louis, MS 39522

DISTRIBUTION (Continued)

Oceanographer of the Navy
Naval Observatory Building 1
Washington, DC 20360

Naval Oceanography Division
Naval Observatory Building 1
ATTN: Code NOP-952 (H. Nicholson)
Washington, DC 20360

Deputy Chief of Naval Operations
ATTN: NOP-211D
Washington, DC 20350

Strategic Systems Project Office
ATTN: SP20123 (P. Fisher)
Washington, DC 20376

Office of Naval Research
800 N. Quincy St.
ATTN: P. C. Badgley
Arlington, VA 22217

Naval Research Laboratory
ATTN: V. Noble
P. Vogt
Washington DC 20375

Commander
Fleet Numerical Oceanography Center
Monterey, CA 93940

Department of the Air Force
HQ Space & Missile Test Center (AFSC)
ATTN: Sven C. Ernbert
Vandenberg Air Force Base, CA 93437

NASA Headquarters
600 Independence Ave., S.W.
ATTN: W. F. Townsend
Washington DC 20546

DISTRIBUTION (Continued)

NASA - Wallops Flight Center
ATTN: J. McGoogan
Wallops Island, VA 23337

NASA - Goddard Space Flight Center
ATTN: J. G. Marsh
R. Kolenkiewicz
Greenbelt, MD 20771

Jet Propulsion Laboratory
4800 Oak Grove Drive
ATTN: W. E. Giberson
P. Rygh
A. Loomis
J. Lorell
G. Born
Pasadena, CA 91103

NOAA - National Ocean Survey/National Geodetic Survey
6001 Executive Blvd.
ATTN: B. H. Chovitz
B. Douglas
C. Goad
Rockville, MD 20852

NOAA - Pacific Marine Environmental Laboratory
ATTN: J. Apel
M. Byrne
Seattle, WA 98105

Aerospace Corporation
2350 East El Segundo Boulevard
ATTN: Library
El Segundo, CA 90245

Applied Physics Laboratory
The Johns Hopkins University
8621 Georgia Avenue
ATTN: John McArthur
C. Kilgus
Silver Spring, MD 20910

DISTRIBUTION (Continued)

University of Texas
Dept. of Aerospace Engineering
ATTN: B. D. Tapley
B. Schultz
Austin, TX 78712

Scripps Institution of Oceanography
ATTN: R. Stewart
R. L. Bernstein
La Jolla, CA 92093

Woods Hole Oceanographic Institute
ATTN: J. A. Whitehead
Woods Hole, MA 02543

Institute of Marine and Atmospheric Science
City University of New York
ATTN: W. J. Pierson
New York, NY 10031

Department of Geodetic Science
Ohio State University
ATTN: R. Rapp
Columbus, OH 43210

Local:

E41	
K05	
K10	
K104 (Ugincius)	
K104 (Zondek)	
K12	(40)
K12 (Groger)	(40)
K12 (Smith, S. L. III)	
K11	
K13	
K14	(5)
X210	(6)


DAT
FILM